IOP Conference Series: Materials Science and Engineering

PAPER • OPEN ACCESS

Preparation of Reduced Graphene Oxide/Magnetic Metal Composites and Its Electromagnetic Wave Absorption Properties

To cite this article: Fuli Yang *et al* 2020 *IOP Conf. Ser.: Mater. Sci. Eng.* **729** 012039

View the article online for updates and enhancements.

You may also like

- A Chemiresistor Sensor Based on Zn_2SnO_4-RGO Hybrids for High Selectivity to ppb-level Oxidizing Gas Under Humidity Conditions
Ziying Wang and Tong Zhang
- Ruthenium-Based Nonaparticles Supported on Ketjenblack/Reduced Graphene Oxide As Air Electrode for Lithium-O_2 Batteries
Xing Xin, Kimihiko Ito and Yoshimi Kubo
- A One-Pot Route for Uniform Deposition of Metal Oxide and Metal Sulfide Nanoparticles on Reduced Graphene Oxide Using Supercritical Alcohols
Jaehoon Kim and Dohyeon Yoon

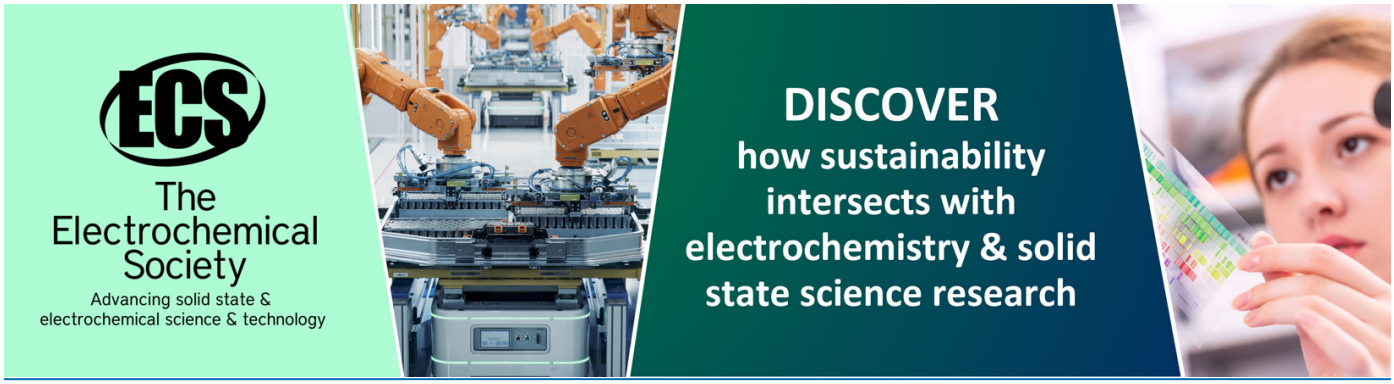

This content was downloaded from IP address 3.143.1.57 on 22/05/2024 at 03:51

Preparation of Reduced Graphene Oxide/Magnetic Metal Composites and Its Electromagnetic Wave Absorption Properties

Fuli Yang[1], Xingzhe Hou[1], Lirui Wang[2], Youjiang Li[2] and Miao Yu[2*]

[1] Electric power research institute, Chongqing Electric Power Corporation, State Grid, Chongqing 401123, China

[2] College of Optoelectronic Engineering, Chongqing University, Chongqing 400044, China

* Corresponding author's e-mail: yumiao@cqu.edu.cn

Abstract: Reduced graphene oxide (RGO) was successfully prepared by reducing graphene oxide (GO) by zinc powder in this paper. Then the reduced graphene oxide (RGO) was combined with Fe and Ni nanoparticles to form RGO/Fe and RGO/Ni composite absorbing materials. The morphology, chemical composition, magnetic properties and electromagnetic parameters of RGO/Fe and RGO/Ni were characterized by means of scanning electron microscopy(SEM), X-ray diffraction(XRD), vibrating sample magnetometry (VSM) and vector network analysis (VNA) to study absorbing mechanism of the as-prepared RGO/magnetic-metal composites, including the effect of magnetic particles Fe and Ni on the absorbing properties. The results showed that in the frequency range of 2-18 GHz, the effective absorption band of RGO/Fe was wider than that of RGO/Ni, with larger reflection loss.

1. Introduction

Recently, microwave technology is developing rapidly in digital equipment and radar detection. Inevitably, electromagnetic radiation came into being. Therefore, the national security problems caused by electromagnetic radiation and electromagnetic environment are also becoming more and more serious. Therefore, it is a key and urgent task to develop electromagnetic absorbing materials that reliably and effectively reduce electromagnetic radiation[1-3].

Graphene is a new type of functional material with low density, large specific surface area, good electrical conductivity, and high dielectric constant. It can make external electrons easily polarize and relax under electromagnetic field and consume electromagnetic waves. Therefore, it has a very good application prospect in the field of electromagnetic protection and electromagnetic stealth[4, 5]. Sang-Eui Lee et al. combined graphite sheet with a volume fraction of 5% with epoxy resin to prepare an absorbing sample, and achieved a reflection loss (RL) of -22 dB at a thickness of 7 mm[6]. Singh et al. mixed 10% of layered porous graphene with nitrile rubber, and the results showed that the graphene/butyronitrile rubber exhibited a very high dielectric loss tangent[7]. However, according to the theory of electromagnetic complementation, single or excessive dielectric loss and magnetic loss are not conducive to the improvement of absorbing performance. The impedance mismatch of graphene is due to the high complex permittivity, which severely limits the microwave absorption properties of graphene[8]. At the same time, absorbing materials with a single loss mechanism are increasingly difficult to meet the ever-expanding microwave frequency band. Wherefore, it is an

Content from this work may be used under the terms of the Creative Commons Attribution 3.0 licence. Any further distribution of this work must maintain attribution to the author(s) and the title of the work, journal citation and DOI.
Published under licence by IOP Publishing Ltd

effective solution to combine graphene with other absorbing mechanism materials to improve impedance matching and enhance electromagnetic wave absorption performance through the synergistic effect of electromagnetic parameters. Soft magnetic metal is an ideal matching material with graphene because of its high magnetic permeability[9]. Due to the adjustable complex permeability and complex permittivity, graphene/magnetic metal has received more and more attention[10].

In this paper, zinc oxide was used to reduce graphene oxide and metal ions by redox method. Graphene oxide reduced by zinc powder was structurally stable, which contained some residual defects and oxygen-containing functional groups. Moreover, it could introduce polarization relaxation and dipole relaxation [11]. In order to reduce the influence of agglomeration on the absorbing properties of composite materials, the thick graphene oxide prepared by Hummer method was used in this paper. Here, two metal elements, Fe and Ni, were selected to study the effects of magnetic metals on graphene composites.

2. Experiment

2.1. Synthesis of graphene@soft magnetic metal nanocomposites

The graphene oxide (GO) was prepared by the modified Hummer method, and the reduced graphene oxide(RGO) suspension was obtained by reducing GO with zinc powder. The average thickness of the RGO was ~19 nm.

The specific steps for preparing RGO/soft magnetic metal nanocomposites were as follows: First, transparent uniform ferric sulfate (FeSO4) solution was prepared by dissolving 5.56 g of FeSO4·7H2O in 400 mL of deionized water. In addition, 60 mg RGO suspension was weighed to added into the above FeSO4 solution, and stirred well until a uniform mixed solution A was obtained. Next, solution B was formed by dissolving 9.07 g of NaBH4 and 0.8 g of NaOH in 240 mL of deionized water, and magnetically stirred for 10 min to evenly mixed. After the above two solutions of A and B were completed, the two mixed solutions A and B were slowly dropped into the reaction tank to carry out reaction. The mixture was allowed to stand for 6 hours to ensure adequate response. After it was fully reacted, the obtained product was vacuum-filtered and dried, then grinded, an RGO/Fe nanocomposite was obtained. Identically, for the goal of obtaining the RGO/Ni nanocomposite, 5.56 g of FeSO4·7H2O was replaced with 5.257 g of NiSO4·6H2O, and the above preparation was repeated.

2.2. Testing and characterization

According to the transmission line theory, for a single-layer absorbing material with a metal backing plate, based on the measured complex permittivity, permeability data and the given thickness, the usual reflection loss (RL) can be calculated by the following formula [1, 12]:

$$Z_{in} = \left(\frac{\mu_0 \mu_r}{\varepsilon_0 \varepsilon_r} \right)^{1/2} \tanh\left(j\left(\frac{2\pi}{c} \right) fd\sqrt{\mu_r \varepsilon_r} \right) \tag{1}$$

$$RL = 20\lg\left| \left(Z_{in} - Z_0 \right) / \left(Z_{in} + Z_0 \right) \right| \tag{2}$$

Where Z_0 is the impedance of free space, Z_{in} is the input impedance between free space and the material interface, c is the speed of light, f is the frequency of the microwave, and d is the thickness of the absorbing material.

The complex permittivity and permeability need to be characterized by vector network analyzer using the coaxial reflection/transmission technique in the 2-18 GHz band. Therefore, paraffin-bonded graphene/magnetic metal composite particles were used to press a ring-shaped sample having an outer diameter of 7 mm, an inner diameter of 3.04 mm, and a thickness of 2 mm, wherein the mass fraction of the composite particles was 40%.

3. Results and discussion

3.1. Characterization of the samples

Spherical magnetic metal nanoparticles were successfully deposited on the surface of the reduced graphene oxide (RGO), and no agglomeration occurred. In the high-power diagram, it could be clearly seen that there were some wrinkles on the RGO film, and the nanoparticles were uniformly grown on the RGO film. The spherical nanoparticles were uniform in size, about 100 nm.

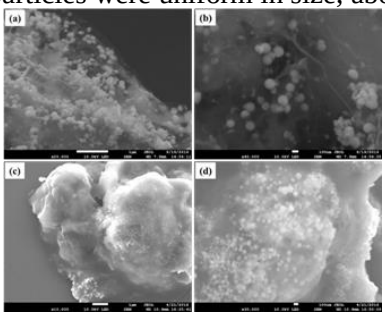

Figure 1. (a), (b) and (c), (d) are the SEM images of RGO/Fe and RGO/Ni nanocomposites.

The XRD pattern of the composite material was shown in figure. 2(a). The diffraction peak of RGO/Fe was located at 2θ=23°and 45°, and diffraction peak at 45°corresponded to the (110) crystal plane of iron. While the diffraction peaks of the RGO/Ni were located at 2θ=23 and 44.8°, and the diffraction peaks at 44.8°matched the nickel (111) crystal plane. The weak diffraction peak at 23°of RGO/Ni and RGO/Fe all corresponded to the RGO (002) crystal plane. Figure. 2(b) showed the hysteresis loop (M-H curve) of RGO/Fe and RGO/Ni at normal temperature. Both materials exhibited typical ferromagnetic properties. The saturation magnetization and coercive force of RGO/Fe were 93.48 emu/g and 76.42 Oe, respectively, while the saturation magnetization and coercive force of RGO/Ni were 3.54 emu/g and 16 Oe, respectively. The magnetic properties of materials were closely related to their morphology, structure, size and crystallinity[13]. The magnetocrystalline anisotropy of the materials can be determined by the value of M_r/M_s[14]. Under the applied electromagnetic field, the magnetocrystalline anisotropy energy of RGO/Fe was 0.039, which was about 3 times that of RGO/Ni. Higher magnetocrystalline anisotropy enabled it to have a larger coercive force *Hc*, and larger *Hc* was often able to make RGO/Fe to obtain a larger imaginary part (μ") of magnetic permeability, which in turn gived RGO/Fe better absorbing properties.

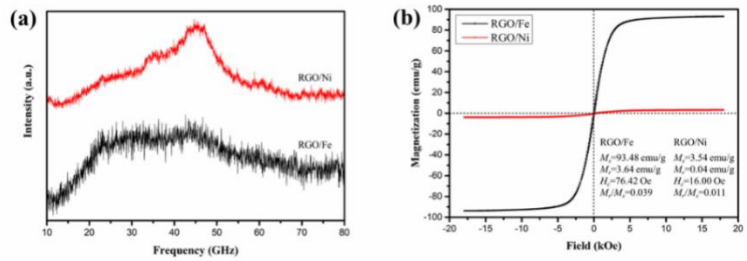

Figure 2. (a) and (b) are the XRD patterns and hysteresis curves of RGO/Fe and RGO/Ni nanocomposites.

3.2. Microwave absorption

It could be obtained from figure. 3 that the real part (ε') and the imaginary part (ε") of permittivity of the two composite materials had large fluctuations in the frequency range of 2-18 GHz. The ε' of RGO/Fe gradually decreased with increasing frequency, which was caused by the polarization lag of the electric dipole. The overall trend of the complex permittivity of RGO/Ni was gradually decreasing with increasing frequency at 2-13 GHz, while large fluctuations appeared at 14-18 GHz. The ε" of

RGO/Fe and RGO/Ni slowly increased with frequency in the low frequency band. After 8 GHz, the ε" of RGO/Fe fluctuated around 4, yet RGO/Ni was fluctuating violently. The fluctuations of the two composite materials at higher frequencies were due to that the dipole moment orientation polarization gradually dominated in the composite material as the frequency increased and the electron polarization was caused by the non-coincidence of the equivalent center.

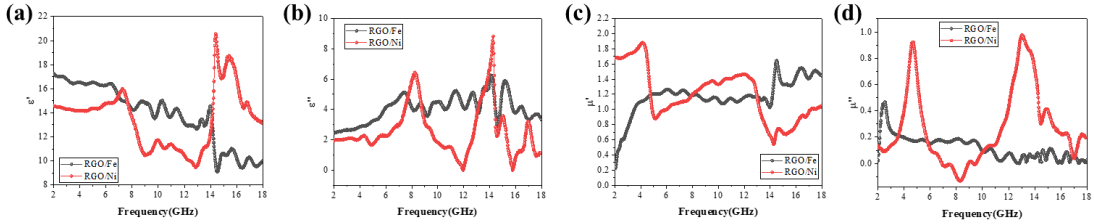

Figure 3. (a) and (b) are the curves of real and imaginary permittivity; (c) and (d) are the curves of the real and imaginary parts of the permeability of RGO/Fe and RGO/Ni with the change of frequency.

The real part (μ') of the complex permeability of RGO/Fe increased first with increasing frequency and then tended to stabilize and then increased, accompanying by slight fluctuations in 5-18 GHz. The μ' of the RGO/Ni magnetic permeability droped sharply at 4-5 GHz and 12.5-14 GHz, and rised slowly in other frequency bands. Whether it was the real part or the imaginary part of the magnetic permeability of RGO/Ni, there were obvious peaks at both the 4 GHz and 13 GHz frequencies. The μ" of RGO/Fe showed a small peak at about 2.5 GHz, which fluctuated slightly in the subsequent bands.

The reflection loss (RL) at different thicknesses was calculated as shown in figure 4. When the thickness of the sample was 2 mm, the maximum reflection loss of RGO/Fe at 9.22 GHz was -25.6 dB, and the effective bandwidth (RL < -10 dB, electromagnetic wave absorption reached 90%) was located at 7.9-11.1 GHz with 3.2 GHz absorption band. As the thickness increased, the absorption peak gradually shifted to the low frequency, movin from 9.22 GHz to 3.6 GHz; and the absorption intensity increased from -25.6 dB at 2 mm to -51.06 dB at 4 mm. The RGO/Ni composite exhibited multiple absorption peaks. When the thickness was 2 mm, it had a broad absorption peak at 8-10 GHz. However, in the 2-18 GHz, the electromagnetic wave absorption was less than -10 dB. When the thickness increased to 3 mm, the maximum reflection loss reached -17.4 dB at 4.44 GHz and the effective bandwidth covered 3.2-7 GHz.

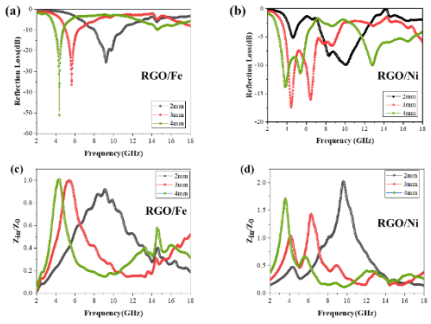

Figure 4. (a) and (b) are respectively the reflection loss curves of RGO/Fe and RGO/Ni with different thickness; (c) (d) are impedance matching curves of RGO/Fe and RGO/Ni with different thickness.

Basic characteristics of electromagnetic absorbing materials: impedance matching and loss capability[15]. The impedance matching (the input impedance of the absorbing material matches the free space impedance) allows the electromagnetic wave to easily enter the material for less reflection. The ideal impedance matching condition is Zin/Z0=1, but it is often not achieved in practice, so often by adjusting Zin/Z0 to be close to 1. It could be seen from figure 4(c) that the best frequency of impedance matching of RGO/Fe at 2-4 mm thickness were 9.22 GHz, 5.9 GHz, and 3.6 GHz, respectively, which corresponded to the frequency of the maximum absorption peak of RGO/Fe.

Meanwhile, it was also found that as the thickness of these samples increases, the frequency with the best impedance matching moved from 9.22 GHz to 3.6 GHz. That was, it moved toward the low frequency, which was consistent with the direction in which the absorption peak moved. From figure 4(d), RGO/Ni had similar results to RGO/Fe.

The dielectric loss tangent （$\tan\delta_\varepsilon$） and magnetic loss tangent （$\tan\delta_\mu$） of the two materials were calculated to further understand the loss mechanism. The RGO/Fe dielectric loss tangent went up with fluctuations in the 2-18 GHz, varying from 0.15 to around 0.5. However, the magnetic loss tangent had a peak at 2.5 GHz and then gradually stabilized around 0.1. It could be inferred that the dielectric loss tangent of RGO/Fe was lower than the magnetic loss tangent in 2-4 GHz, while the dielectric loss in the 4-18 GHz was the main loss mechanism. The RGO/ Ni dielectric loss tangent and the magnetic loss tangent curves had two sharp peaks in the whole test frequency band.

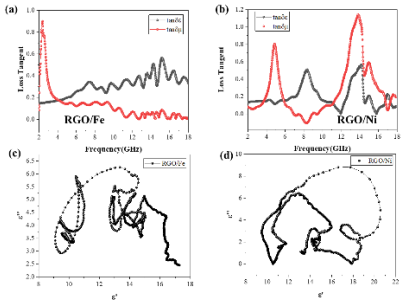

Figure 5. (a) and (b) are tangent curves of dielectric loss and magnetic loss of RGO/Fe and RGO/Ni nanocomposites；(c) and (d) are RGO/Fe and RGO/Ni col-cole semicircle; (e) is the value of C0 of RGO/Fe and RGO/Ni nanocomposites changes with frequency curve.

As is well known, Dielectric loss includes the extremely important loss mechanism of Debye relaxation [16, 17]. From the transmission line theory, the complex permittivity can be expressed by the following formula [18, 19]：

$$\left(\varepsilon'-\frac{\varepsilon_s+\varepsilon_\infty}{2}\right)^2+\left(\varepsilon''\right)^2=\left(\frac{\varepsilon_s-\varepsilon_\infty}{2}\right)^2 \quad (3)$$

Where τ, ε_∞ and ε_s are the polarization relaxation time, the permittivity in optical frequency and the static dielectric constant, respectively. Each Cole-Col semicircle corresponded to a Debye process[20]. These relaxation processes resulted from the migration of carriers between the reduced graphene oxide and the magnetic metal particles, and interfacial polarization, which was due to the accumulation of a large amount of charge between particles and paraffin. Both samples had multiple Cole-Cole semicircles. Compared with RGO/Ni, the Cole-Cole semicircle of RGO/Fe was obviously distorted. These curves showed that in addition to the Debye relaxation process, residual defects in RGO and oxygen-containing functional groups could accumulate electrons which caused electron polarization to form dielectric relaxation.

4. Conclusion

In this paper, RGO/Fe and RGO/Ni nanocomposites were successfully prepared by zinc oxide reduction of graphene oxide and metal ions. The effects of morphology, electromagnetic parameters, impedance matching and Debye relaxation on the absorbing properties were systematically investigated. At a certain thickness, the absorption peaks of RGO/Fe and RGO/Ni are at the best impedance matching frequency. As the thickness increases, absorption peak moved to the low frequency band as well as impedance matching frequency. Meanwhile, due to the large coercive force, good impedance matching and strong loss capability of RGO/Fe, electromagnetic waves could enter the absorbing material as much as possible to induce large attenuation. The visual representation was that the RGO/Fe absorption band was wider with better absorbing performance.

Acknowledgments
The financial support from Electric power research institute of Chongqing Electric Power Corporation of State Grid (52202317001D) is highly acknowledged.

References
[1] Li, X., Feng, J., Du, Y., et al. (2015) One-pot synthesis of CoFe2O4/graphene oxide hybrids and their conversion into FeCo/graphene hybrids for lightweight and highly efficient microwave absorber[J]. Journal of Materials Chemistry A., 3(10): 5535-5546.
[2] Lee, S., Jo, I., Kang, S., et al. (2017) Smart Contact Lenses with Graphene Coating for Electromagnetic Interference Shielding and Dehydration Protection[J]. ACS Nano., 11(6): 5318-5324.
[3] Lin, Y., Dong, J., Zong, H., et al. (2018) Synthesis, Characterization, and Electromagnetic Wave Absorption Properties of Composites of Reduced Graphene Oxide with Porous LiFe5O8 Microspheres[J]. ACS Sustainable Chemistry & Engineering., 6(8): 10011-10020.
[4] Li, Y., Yu, M., Yang, P., et al. (2017) Enhanced Microwave Absorption Property of Fe Nanoparticles Encapsulated within Reduced Graphene Oxide with Different Thicknesses[J]. Industrial & Engineering Chemistry Research., 56(31): 8872-8879.
[5] Wang, G., Zhang, X., Wei, Y., et al. (2013) Polymer composites with enhanced wave absorption properties based on modified graphite and polyvinylidene fluoride[J]. Journal of Materials Chemistry A., 1(24):7031.
[6] Lee, S., Choi, O., Hahn, H., (2008) Microwave properties of graphite nanoplatelet/epoxy composites[J]. Journal of Applied Physics., 104(3): 33705.
[7] Singh, V., Shukla, A., Patra, M., et al. (2012) Microwave absorbing properties of a thermally reduced graphene oxide/nitrile butadiene rubber composite[J]. Carbon., 50(6): 2202-2208.
[8] Gupta, A., Singh, A., Varshney, S., et al. (2014) New insight into the shape-controlled synthesis and microwave shielding properties of iron oxide covered with reduced graphene oxide[J]. RSC Adv., 4(107): 62413-62422.
[9] Luo, P., Liu, Z., Tao, R., et al. (2018) Design of double-layered flaky carbonyl iron/polyurethane wave-absorbing coating and its electromagnetic properties[J]. Electroplating & Finishing, 6: 247-253.
[10] Kong, L., Yin, X., Xu, H., et al. (2019) Powerful absorbing and lightweight electromagnetic shielding CNTs/RGO composite[J]. Carbon., 145: 61-66.
[11] Xu, S., Chen, G., Zhang, H., et al. (2016) Preparation and Electromagnetic Absorption Performance of Ni-RGO[J]. Journal of Inorganic Materials, 6: 567-574.
[12] Saini, L., Patra, M., Dhaka, M., et al. (2018) Ni/graphitic carbon core–shell nanostructure-based light weight elastomeric composites for Ku-band microwave absorption applications[J]. CrystEngComm., 20(32): 4630-4640.
[13] Wang, Z., Bi, H., Wang, P., et al. (2015) Magnetic and microwave absorption properties of self-assemblies composed of core–shell cobalt–cobalt oxide nanocrystals[J]. Phys. Chem. Chem. Phys., 17(5):3796-3801.
[14] Yan, S., (2011). Structure and Electromagnetic Properties of Ferromagnetic Metal Micro/Nanoparticles Covered by Dielectric Layer[D]. Harbin Institute of Technology, Harbin.
[15] Xie, P., Li, H., He, B., et al. (2018) Bio-gel derived nickel/carbon nanocomposites with enhanced microwave absorption[J]. Journal of Materials Chemistry C., 6(32): 8812-8822.
[16] Guo, F., Du, H., Qu, S., et al. (2015) Oxidation resistance and microwave absorption property of core shell urchin-like ZnO\Carbonyl iron powder composite particles[J]. Chinese Journal of Inorganic Chemistry, 4: 755-760.
[17] Zhao, B., Shao, G., Fan, B., et al. (2015) Synthesis of flower-like CuS hollow microspheres based on nanoflakes self-assembly and their microwave absorption properties[J]. JOURNAL OF MATERIALS CHEMISTRY A., 3(19): 10345-10352.

[18] Zhu, W., Wang, L., Zhao, R., et al. (2011) Electromagnetic and microwave-absorbing properties of magnetic nickel ferrite nanocrystals[J]. NANOSCALE., 3(7): 2862-2864.
[19] Zhao, B., Shao, G., Fan, B., et al. (2015) Synthesis of flower-like CuS hollow microspheres based on nanoflakes self-assembly and their microwave absorption properties[J]. J. Mater. Chem. A. 2015, 3(19): 10345-10352.
[20] Du, Y., Liu, W., Qiang, R., et al. (2014) Shell Thickness-Dependent Microwave Absorption of Core–Shell Fe3O4@C Composites[J]. ACS Applied Materials & Interfaces., 6(15): 12997-13006